RESEARCH ARTICLE

Potassium bisperoxo (1,10-phenanthroline) oxovanadate suppresses proliferation of hippocampal neuronal cell lines by increasing DNA methyltransferases

Xiao-Li Tian[1, 2, 3, #], Shu-Yuan Jiang[1, 2, #], Xiao-Lu Zhang[1, 2, 3, #], Jie Yang[1, 2], Jun-He Cui[1, 2], Xiao-Lei Liu[1, 2], Ke-Rui Gong[4], Shao-Chun Yan[1, 2], Chun-Yang Zhang[5, *], Guo Shao[1, 2, 3, *]

1 Biomedicine Research Center, Basic Medical College and Baotou Medical College of Neuroscience Institute, Baotou Medical College, Baotou, Inner Mongolia Autonomous Region, China
2 Inner Mongolia Key Laboratory of Hypoxic Translational Medicine, Baotou Medical College, Baotou, Inner Mongolia Autonomous Region, China
3 Beijing Key Laboratory of Hypoxic Conditioning Translational Medicine, Xuanwu Hospital, Capital Medical University, Beijing, China
4 Department of Oral and Maxillofacial Surgery, University of California San Francsico, San Francisco, CA, USA.
5 Department of Neurosurgery, the First Affiliated Hospital of Baotou Medical College, Baotou, Inner Mongolia Autonomous Region, China

Funding: *This study was supported by the National Natural Science Foundation of China, No. 81160244, 81360316, 81460283, 81660307 (all to GS); the Inner Mongolia Science Foundation of China, No. 2018LH08078 (to GS), 2016MS(LH)0307 (to SYJ); the Baotou Health Foundation, China, No. WSJJ2016008 (to SYJ); the Inner Mongolia Educational Research Foundation of China, No. NJZY207 (to GS), NJZY17243 (to SCY), NJZY17250 (to XLL), NJZY17251 (to SYJ); the Baotou Medical College Foundation of China, No. BYJJ-DF201602, BYJJ-YF201615, BSJJ201617, BYJJ-QM201633, BYJJ-QM201656, BYJJ201502 (to GS); the Science and Technology Planning Project of Baotou of China, No. CX2017-5 (to GS); the National Key R&D Program of China, No. 2017YFC1308405 (to GS).*

Graphical Abstract

Potassium bisperoxo (1,10-phenanthroline) oxovanadate (BpV (phen)) increases the expression of DNA methyltransferases (DNMTs) which may be related to cell cycle arrest and p21 increase

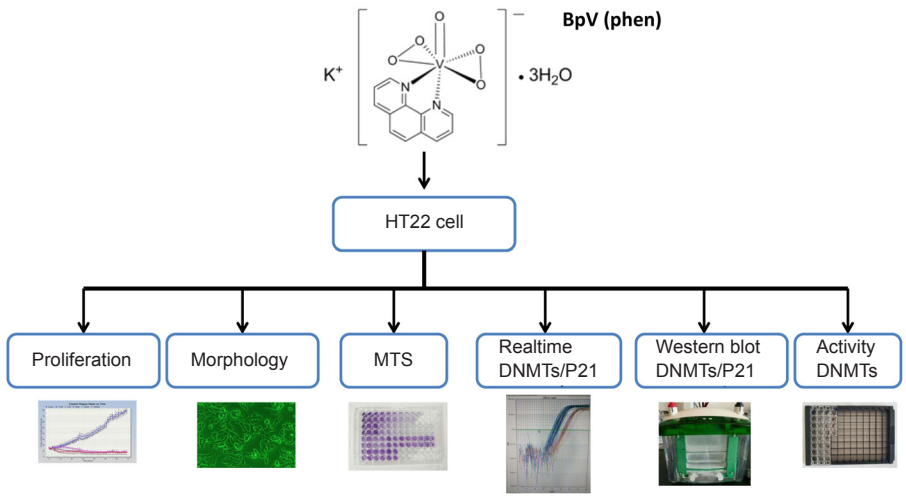

Correspondence to:
Guo Shao, MD, shao_guo_china@163.com;
Chun-Yang Zhang, zhangchunyangbyyfy@163.com.

#These authors contributed equally to this work.

orcid:
0000-0003-3766-5076 (Guo Shao)
0000-0002-0310-0205 (Chun-Yang Zhang)

doi: *10.4103/1673-5374.249230*

Received: *June 4, 2018*
Accepted: *September 25, 2018*

Abstract

Bisperoxo (1,10-phenanthroline) oxovanadate (BpV) can reportedly block the cell cycle. The present study examined whether BpV alters gene expression by affecting DNA methyltransferases (DNMTs), which would impact the cell cycle. Immortalized mouse hippocampal neuronal precursor cells (HT22) were treated with 0.3 or 3 μM BpV. Proliferation, morphology, and viability of HT22 cells were detected with an IncuCyte real-time video imaging system or inverted microscope and 3-(4,5-dimethylthiazol-2-yl)-5(3-carboxymethonyphenol)-2-(4-sulfophenyl)-2H-tetrazolium, respectively. mRNA and protein expression of DNMTs and p21 in HT22 cells was detected by real-time polymerase chain reaction and immunoblotting, respectively. In addition, DNMT activity was measured with an enzyme-linked immunosorbent assay. Effects of BpV on the cell cycle were analyzed using flow cytometry. Results demonstrated that treatment with 0.3 μM BpV did not affect cell proliferation, morphology, or viability; however, treatment with 3 μM BpV decreased cell viability, increased expression of both DNMT3B mRNA and protein, and inhibited the proliferation of HT22 cells; and 3 μM BpV also blocked the cell cycle and increased expression of the regulatory factor p21 by increasing DNMT expression in mouse hippocampal neurons.

Key Words: *nerve regeneration; hippocampal neurons; potassium bisperoxo (1,10-phenanthroline) oxovanadate; DNA methyltransferase; p21; HT22 cell; cell cycle; immunoblotting; DNA methylation; neural regeneration*

Chinese Library Classification No. *R453; R364*

Introduction

Vanadium can adopt multiple oxidation states and different vanadium compounds have arisen as potential drugs for their anti-diabetic, anti-cancer, and anti-parasitic effects (Kioseoglou et al., 2015; Irving and Stoker, 2017; Levina and Lay, 2017). Potassium bisperoxo (1,10-phenanthroline) oxovanadate (BpV), a V^{5+} compound and specific inhibitor of protein tyrosine phosphatases, can arrest the cell cycle and alter neurotransmitter release in nerve cells (Faure et al., 1995; Bieger et al., 2002). Jung and his colleagues reported that vanadium can alter DNA methylation levels of some genes (Jung et al., 2017). DNA methylation, which is governed by methyltransferases (DNMTs), can regulate gene expression to ultimately determine the characteristics of a cell (Bestor, 2000; Rodriguez-Osorio et al., 2010; Taberlay and Jones, 2011). Thus, changes in DNMTs may account for the biological function of vanadium, which can serve as a potential drug. Indeed, changes in DNMT and DNA methylation levels of cell cycle-related genes may be potential mechanisms of As_2O_3-induced cell cycle arrest (Eyvani et al., 2016). Moreover, DNA methylation patterns can alter expression of some neurotransmitter genes (Alelu-Paz et al., 2014) and DNMT-catalyzed DNA methylation is one mechanism by which gene expression is regulated in the brain (Gibbs et al., 2010; Bettscheider et al., 2012; Zhang et al., 2014; Yu et al., 2017). The aim of this study was to explore whether BpV affects DNMTs, which regulate DNA methylation patterns.

DNA methylation is catalyzed by three active DNMTs (DNMT1, DNMT3A, and DNMT3B) and one non-catalytic accessory protein (DNMT3L). DNA methylation takes place at position five of cytosine residues in CpG islands (Bestor, 2000; Shao et al., 2013; Liu et al., 2017). Establishing specific DNA methylation patterns is important for both normal or abnormal cell processes, such as somatic tissue development and cancer (Okano et al., 1999; Cassinotti et al., 2012; Cheng et al., 2014; Saradalekshmi et al., 2014). DNMTs also play important roles in cell cycle control (Stephens et al., 1996; Xiong et al., 2009; Yang et al., 2017). Fournel et al. (1999) showed that DNMT inhibition upregulated protein levels of p21, a cell cycle regulator. Fang and Lu (2002) reported that p21 may be a key factor in the growth arrest induced in transformed cells. This study explored the effects of BpV on DNMTs and the cell cycle (*via* detection of p21, a cyclin-dependent kinase inhibitor) in immortalized mouse hippocampal neuronal precursor cells (HT22).

Materials and Methods

Cell culture and treatment with BpV

HT22 cells (National Laboratory of Molecular Oncology, Cancer Institute and Hospital, Chinese Academy of Medical Sciences and the Peking Union Medical College, China) were maintained in our laboratory as previously described (Zhao et al., 2016). Cells were either treated with vehicle (0.1% dimethyl sulfoxide) (Sigma, St. Louis, MO, USA) or BpV (Alexis, San Diego, CA, USA). The pH value of cell culture medium was 7 and BpV is stable in neutral aqueous solution (Matsugo et al., 2015; Chakrabarty and Banerjee, 2016).

IncuCyte assays

HT22 cells were seeded in 96-well tissue culture plates at a density of 4000 cells per well. Wells were randomly divided into six groups and cultured for 24 hours before adding BpV at concentrations of 0, 0.3, 3, 30, 300, or 3000 μM (n = 3). Cells were cultured for 12 hours and then treated with BpV at various concentrations or 0.1% dimethyl sulfoxide as a control. Cells were monitored and imaged with an IncuCyte FLR, and data were analyzed with IncuCyte Confluence version 1.5 software (Essen Bioscience, Ann Arbor, MI, USA). All experiments were performed in triplicate.

3-(4,5-Dimethylthiazol-2-yl)-5(3-carboxymethonyphenol)-2-(4-sulfophenyl)-2H-tetrazolium (MTS) assay

Cell viability was measured by MTS assay using a CellTiter 96 Aqueous One Solution Cell Proliferation Assay kit (Promega, Madison, WI, USA). According to the manufacturer's protocol, cells were seeded into 96-well plates and treated with BpV or dimethyl sulfoxide. HT22 cells were seeded into a 96-well plate at a density of 2000 cells per well and cultured in an incubator with 5% CO_2 and 95% air at 37°C for 24 hours. Different concentrations of BpV or dimethyl sulfoxide were added for 24 hours. MTS was added and detected every half hour. Experiments were performed as previously described by Hwang et al. (2011). Each experiment was conducted in triplicate.

Real time-polymerase chain reaction (PCR)

HT22 cells were cultured to 70% confluence in culture dishes with 5% CO_2 and 95% air at 37°C. BpV (0.3 or 3 μM) was added for 12 or 24 hours. Total RNA was extracted from HT22 cells with or without BpV treatment using Trizol reagent (Invitrogen, Carlsbad, CA, USA) according to the manufacturer's instructions. The concentration and purity of RNA were determined spectrophotometrically by reading the absorbance at 260 and 280 nm. Aliquots (3 μg) of total RNA were reverse transcribed into cDNA using a commercial kit (Invitrogen). Real time-PCR was conducted in triplicate on an ABI 7900 real-time PCR system using PowerUP SYBR green master mix (Thermo Fisher Scientific, San Jose, CA, USA), a Quant Studio 7 Flex instrument, and fast gene-expression method with the following cycling conditions: 95°C for 2 minutes; 40 cycles of 95°C for 30 seconds, 59°C for 30 seconds, and 72°C for 30 seconds; followed by 72°C for 2 minutes. Reactions were carried out in triplicate and β-actin gene expression was used as an internal control to normalize variability in expression levels. The results were analyzed by the $2^{-\Delta\Delta CT}$ value method, as previously described (Zhang et al., 2014, 2016). Primers used in this study are shown in **Table 1**.

Table 1 Primer sequences

	Sequence (5′–3′)	Product (bp)
DNMT1	Forward: CCT GGC TAA AGT CAA GTC CCT	60
	Reverser: GTG TGT GTT CCG TTC TCC AAG	
DNMT3A	Forward: GGC CGA ATT GTG TCT TGG TG	80
	Reverser: CCA TCT CCG AAC CAC ATG AC	
DNMT3B	Forward: AAG CTC CCG GCT GTC TAA GA	52
	Reverser: CTG CGT GTA ATT CAG AAG GCT	
P21	Forward: CCT GGT GAT GTC CGA CCT G	106
	Reverser: CCA TGA GCG CAT CGC AAT C	
β-Actin	Forward: GGC TGT ATT CCC CTC CAT CG	154
	Reverser: CCA GTT GGT AAC AAT GCC ATG T	

DNMT1: DNA (cytosine-5)-methyltransferase 1; DNMT3A: DNA (cytosine-5)-methyltransferase 3A; DNMT3B: DNA (cytosine-5)-methyltransferase 3B; P21: cyclin-dependent kinase inhibitor 1A.

Immunoblotting

HT22 cells were cultured to 70% confluence in culture dishes with 5% CO_2 and 95% air at 37°C. BpV (0.3 or 3 μM) was added for 12 or 24 hours. After harvesting, cells were washed in phosphate-buffered saline before lysing with radioimmunoprecipitation assay buffer (Beyotime Biotechnology, Shanghai, China). Protein concentrations were determined using a bicinchoninic acid protein assay kit (Pierce Biotechnology, Rockford, IL, USA). Equal amounts of protein were separated by 10% sodium dodecyl sulfate polyacrylamide gel electrophoresis and transferred to nitrocellulose membranes (Roche Diagnostics, Indianapolis, IN, USA). Membranes were blocked with 5% nonfat milk before incubation with rabbit polyclonal anti-DNMT1, -DNMT3A, -DNMT3B, or -P21 (a cyclin-dependent kinase inhibitor) (Novus Biologicals, Littleton, CO, USA), and a mouse monocloncal anti-actin antibody (Sigma) (Liu et al., 2017). Primary antibodies were used at a dilution of 1:1000. Blots were visualized with an enhanced chemiluminescence detection system (Beyotime Biotechnology). Optical densities of bands were quantified using ImageJ 1.8.0 software (Scion Corporation, Torrance, CA, USA). Western blot data were normalized to β-actin. Cells were harvested and lysed. Protein expression levels of DNMT1, DNMT3A, DNMT3B, and p21 were determined by immunoblotting analysis as previously described by He et al. (2013).

Analysis of cell cycle

HT22 cells were cultured to 70% confluence in culture dishes with 5% CO_2 and 95% air at 37°C. BpV (0.3 or 3 μM) was added for 12 or 24 hours. Cell cycle distribution was measured with flow cytometry (Becton Dickinson, Franklin Lakes, NJ, USA). Briefly, cells were cultured as previously described, collected, and washed twice in phosphate-buffered saline. Cell pellets were re-suspended in 0.5 mL phosphate-buffered saline and fixed in 4.5 mL 70% ethanol overnight. The following day, cells were centrifuged at 800 × *g* for 5 minutes and pellets were resuspended in 0.1% Triton X-100 containing 0.2 mg/mL propidium iodide and 0.1 mg/mL RNase A. This was followed by incubation in the dark for 30 minutes at room temperature (Yang et al., 2017). Cells were cultured, fixed, and stained as previously described (Yang et al., 2017). Percentages of cells in each phase of the cell cycle (G_0/G_1, S, and G_2/M) were analyzed using ModFit 3.0 software (Becton Dickinson). Cell percentages were calculated as previously described by Bohmer (1982). Results are reported as percentages of total cells in each phase.

DNMT activity assay

HT22 cells were cultured to 70% confluence in culture dishes with 5% CO_2 and 95% air at 37°C. BpV (0.3 or 3 μM) was added for 12 or 24 hours. Nuclear proteins were isolated with and EpiQuik nuclear extraction kit (Epigentek, Brooklyn, NY, USA). The reaction was initiated by adding 10 μg of nuclear extracts to the unique, cytosine-rich DNA substrate coated enzyme-linked immunosorbent assay (ELISA) plate provided in the EpiQuik DNMT Activity/Inhibition Assay Ultra Kit (Epigentek), which contains active DNMTs, and incubating for 60 minutes at 37°C. Methylated DNA was recognized by an anti-5-methylcytosine antibody. Amounts of methylated DNA, which is proportional to enzyme activity, were calorimetrically quantified at 450 nm (Yang et al., 2017).

Statistical analysis

Data are expressed as the mean ± SD and were analyzed with SPSS Version 17.0® software (SPSS, Chicago, IL, USA). One-way analysis of variance followed by Tukey's honest significant difference *post hoc* test was applied for statistical analysis. $P < 0.05$ was considered statistically significant.

Results

Effect of BpV on cell proliferation and viability

Results of incubation of HT22 cells with BpV at various concentrations from 0.3 μM (0.1 μg/mL) to 3 mM (1 mg/mL) are presented in **Figure 1A**. A concentration of 0.3 μM BpV did not affect the proliferation of HT22 cells. However, treatment with 3 μM (1 μg/mL) BpV completely arrested cell proliferation. These results indicated that 3 μM was the lowest concentration at which cell proliferation was totally arrested in this study. HT22 cell viability was detected at 12 and 24 hours after BpV treatment with concentrations ranging from 0.3 μM to 3 mM (**Figure 1B** and **C**). Lower dosages of BpV (0.3 μM) were unable to remarkably decrease cell viability at 12 or 24 hours after treatment. Moreover, 3 μM BpV decreased cell viability at 24 hours, but showed no significant effect at 12 hours. Therefore, 0.3 μM and 3 μM BpV were used in subsequent experiments.

Effect of BpV on cell morphology

HT22 cells treated with vehicle showed good refraction with sharp and clear membrane borders by light micros-

copy (**Figure 2**). After 12 or 24 hours of exposure to 3 μM BpV, the morphological appearance of HT22 cells was obviously changed, along with a reduction in cell number and increase in cellular debris, indicating reduced cell viability. However, the morphological appearance of cells incubated with 0.3 μM BpV was not obviously changed with regard to cell number or cellular debris.

Influence of BpV on cell cycle

The effect of BpV on cell cycle is shown in **Figure 3**. BpV at a concentration of 0.3 μM did not markedly affect cell cycle phases. However, incubation with 3 μM BpV for 24 hours arrested the cell cycle in S phase ($P < 0.05$).

Effect of BpV on DNMT expression levels

HT22 cells were incubated with 0.3 μM or 3 μM BpV for 12 or 24 hours. DNMT1, DNMT3A, and DNMT3B mRNA were significantly increased at 12 and 24 hours (**Figure 4A–F**) with 3 μM BpV. However, with regard to protein levels, only DNMT3B was found to be increased at 24 hours in the 3 μM BpV group (**Figure 4M**). Notably, 0.3 μM BpV did not produce any significant alterations of DNMT mRNA or protein expression levels (**Figure 4**).

Influence of BpV on DNMT activity

Total DNMT activities were detected with an EpiQuik DNMT Activity/Inhibition Assay Ultra Kit. At a concentration of 0.3 μM, BpV did not significantly affect DNMT activities. However, at a concentration of 3 μM BpV, DNMT activities were significantly increased at 24 hours ($P < 0.05$; **Figure 4N**).

Influence of BpV on p21 expression

Results shown in **Figure 5** demonstrate that 3 μM BpV remarkably increased mRNA and protein expression levels of p21 at 24 hours. However, 0.3 μM BpV did not produce any notable alteration in p21 mRNA or protein expression levels (**Figure 5**).

Discussion

BpV is well known for its protein tyrosine phosphatase inhibitor function, insulin-mimetic properties, and anti-tumor activity (Posner et al., 1994; Bevan et al., 1995; Caron et al., 2008). Additionally, it has effects on nerve cells in animal and cell models. BpV showed neuroprotective effects on the function of primary sensory axons (Nakashima et al., 2008). In addition, it can enhance dopamine release, a neurotransmitter produced by neurons, in PC12 cells (Bieger et al., 2002). In the present study, we explored the effect of BpV on DNMTs in HT22 cells, a mouse hippocampus-derived cell line that is widely used as an *in vitro* neural cell model. Our results showed that treatment with 3 μM BpV completely blocked the proliferation of HT22 cells. Expression of DNMTs and p21 was increased, and cells were blocked at the S transition of mitosis.

Different concentrations of BpV were administered to neural cells *in vitro* or *in vivo*. Cerovac et al. (1999) reported that 0.1 μM BpV was not toxic to the rat neural cell line PC12, and 5–10 μM BpV did not cause a significant amount of death; however, 100 μM BpV was toxic to PC12 cells. Rats infused with 3 or 10 μM BpV exhibited reduced 6-hydroxydopamine-induced neurotoxic injury in rat nigrostriatal neurons (Yang et al., 2007). Similarly, different concentrations of BpV had different effects on HT22 cells: 0.3 μM BpV did not affect proliferation, while 3 μM BpV completely inhibited proliferation. Nevertheless, HT22 cells treated with 3 μM BpV exhibited inhibited proliferation, with fewer cells and more cellular debris.

Inhibition of HT22 cell profileration by BpV may result from cell cycle arrest. We previously reported that the cell cycle of EC109 cells incubated with 100 μM vanadium compound (NaV) was arrested at S phase (Yang et al., 2016). Moreover, the cell cycle progression of neuroblastoma and glioma cells was arrested by BpV at the G2/M phase (Faure et al., 1995). In the present study, HT22 cells were arrested at S phase by 3 μM BpV. Thus, different types of cells may show different sensitivities to BpV, which may arrest cells at different cell cycle phases.

Notably, the cell cycle arrest effect induced by BpV could be caused by reactive oxygen species (Andrezalova et al., 2013). Indeed, Matsugo et al. (2015) reported that peroxidovanadium complexes can generate reactive oxygen species, which may induce upregulation of DNMT expression (Wu and Ni, 2015; Tasdogan et al., 2016; Miozzo et al., 2018). It has also been suggested that Cr(IV)-induced G1 phase arrest may contribute to global hypomethylation (Lou et al., 2013). Notably, silver nanoparticles (AgNPs) can induce G2/M phase arrest and increase DNMT expression in HT22 cells (Mytych et al., 2017). However, the relationship between DNMTs and BpV has not been reported thus far. We proposed that BpV may be similar to Cr(IV) and AgNPs, which can induce changes in DNA methylation and DNMT expression to elicit cytotoxic effects. Although we did not detect DNA methylation levels directly, we measured DNMT expression and activity in HT22 cells after BpV treatment and found that BpV may affect the HT22 cell epigenome by increasing levels of DNMT1, DNMT3A, and DNMT3B. Decitabine treatment increased the percentage of cells in G2/M and upregulated p21 expression independent of DNMT1 and DNMT3b in leukemia cells (Jiemjit et al., 2008). As such, DNMT expression and activities may underlie the mechanisms responsible for cell cycle arrest.

Elevated expression of p21 may play a vital role in cellular growth arrest (Yu et al., 2009; Zurlo et al., 2013; Li et al., 2014). After BpV treatment, p21 levels increased, which may contribute to the BpV-mediated anti-proliferative activity observed in our study. We found that both DNMTs and p21 were increased in HT22 cells after treatment with 3 μM BpV. Notably, a GC-rich region has been reported in the human p21 promoter (Prowse et al., 1997; Fang and Lu, 2002). Therefore, increased DNMT expression may lead to gene hypermethylation and decreased gene expression.

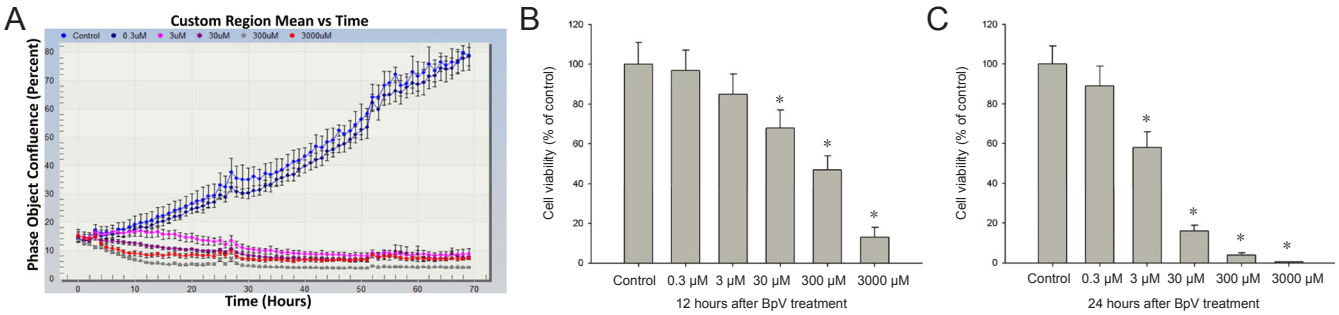

Figure 1 Proliferation and viability of cells treated with different concentrations of BpV.
(A) HT22 cells were treated with a serial dilution of BpV for 72 hours. Growth rates were measured using an IncuCyte real-time video imaging system. (B, C) Cell viability, as assessed by MTS assay, was expressed as a percentage of the control and calculated as: $OD_{treated}/OD_{control} \times 100\%$. $*P < 0.05$, *vs.* control. Data are expressed as the mean ± SD (six well-independent experiments, one-way analysis of variance followed by Tukey's honest significant difference *post hoc* test). Experiments were performed in triplicate. BpV: Bisperoxo (1,10-phenanthroline) oxovanadate; MTS: 3-(4,5-dimethylthiazol-2-yl)-5(3-carboxymethonyphenol)-2-(4-sulfophenyl)-2H-tetrazolium; OD: optical density.

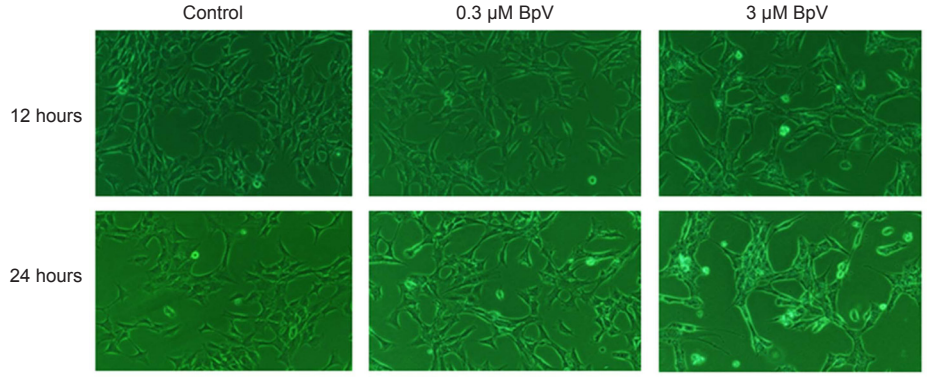

Figure 2 Morphological appearance of HT22 cells treated with 0.3 or 3 μM BpV for 12 or 24 hours.
Morphological changes were observed under an inverted microscope (magnification, 100×). BpV: Bisperoxo (1,10-phenanthroline) oxovanadate.

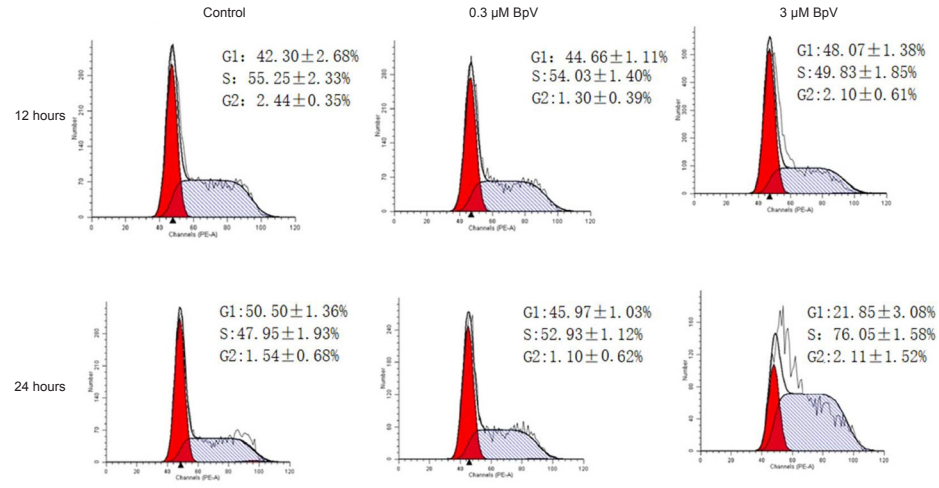

Figure 3 Flow cytometry analysis of the cell cycle in HT22 cells treated with BpV.
HT22 cells were treated with dimethyl sulfoxide vehicle (control) or 0.3 or 3 μM BpV for 12 or 24 hours. The cell cycle was analyzed with propidium iodide staining and flow cytometry. Representative data of experiments performed in triplicate are shown. BpV: Bisperoxo (1,10-phenanthroline) oxovanadate.

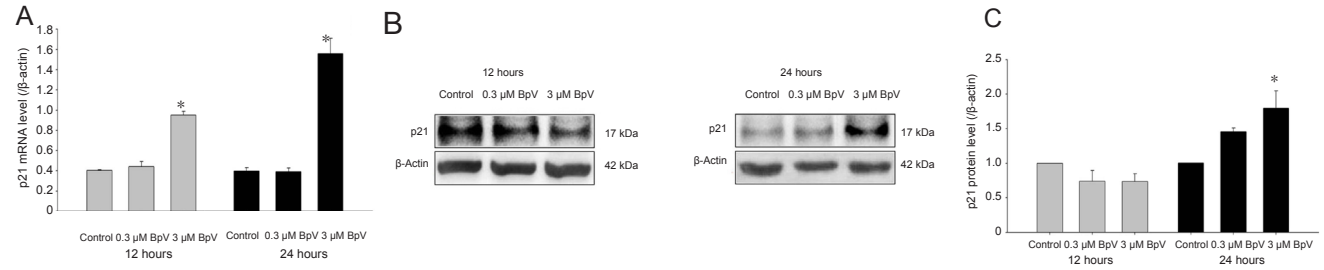

Figure 5 BpV increases the expression of p21 (a cyclin-dependent kinase inhibitor) in HT22 cells.
HT22 cells were treated with dimethyl sulfoxide vehicle (control) or 0.3 or 3 μM BpV for 12 or 24 hours. (A) mRNA level of p21. (B) Representative result of immunoblotting indicating expression of p21 protein. (C) Semi-quantitative analysis indicated changes in p21 levels. p21 mRNA abundance was measured by real time-polymerase chain reaction, while p21 protein abundance was measured by immunoblotting. $*P < 0.05$, *vs.* control. Data are expressed as the mean ± SD (six-well independent experiments, one-way analysis of variance followed by Tukey's honest significant difference *post hoc* test). Experiments were performed in triplicate. BpV: Bisperoxo (1,10-phenanthroline) oxovanadate.

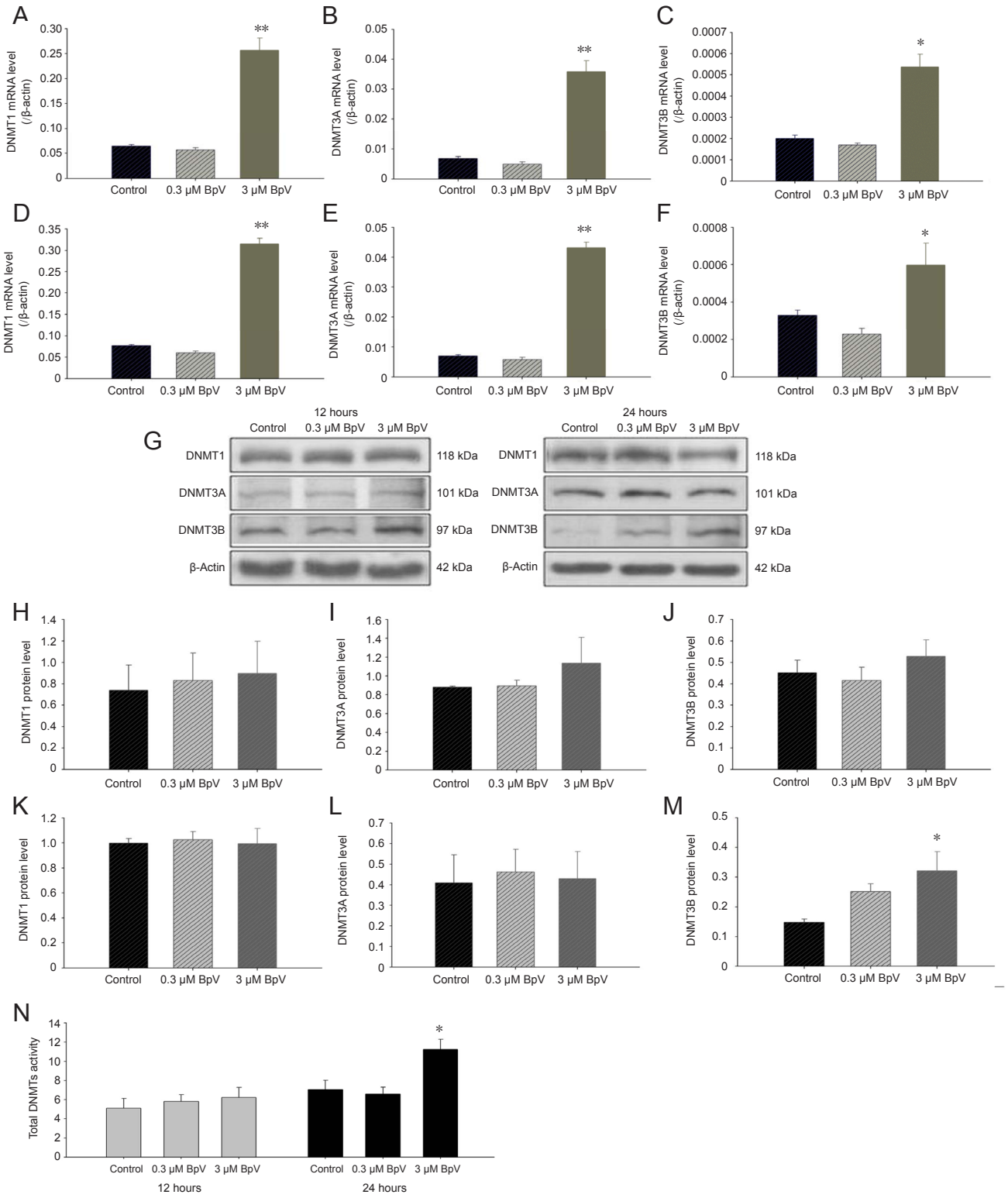

Figure 4 Effect of BpV on expression and activity of DNMTs in HT22 cells across time.

HT22 cells were treated with dimethyl sulfoxide vehicle (control) or 0.3 or 3 BpV for 12 or 24 hours. mRNA levels of DNMT1, DNMT3A, and DNMT3B at 12 hours (A–C) and (D–F) 24 hours. (G) Representative results of immunoblotting showing expression of DNMT1, DNMT3A, and DNMT3B at 12 and 24 hours. Semi-quantitative analysis indicated changes in levels of DNMT1, DNMT3A, and DNMT3B at 12 hours (H–J) and 24 hours (K–M). (N) Total activity of DNMTs (12 or 24 hours). DNMT1, DNMT3A, and DNMT3B mRNA abundance was measured by real time-polymerase chain reaction; beta-actin was used as a control. DNMT1, DNMT3A, and DNMT3B protein abundance was measured by immunoblotting and signals were quantified by densitometry. DNMT activity was measured by enzyme-linked immunosorbent assay. $*P < 0.05$, $**P < 0.01$, *vs.* control. Data are expressed as the mean ± SD (six-well independent experiments, one-way analysis of variance followed by Tukey's honest significant difference *post hoc* test). Experiments were performed in triplicate. BpV: Bisperoxo (1,10-phenanthroline) oxovanadate; DNMT: DNA methylation.

However, Fournel et al. (1999) demonstrated a regulatory link between DNMT and p21 that was independent of DNA methylation. Thus, BpV-induced increases in p21 may not depend on changes of its promoter DNA methylation. Results for p21 were consistent with the findings of Fournel and colleagues (Fournel et al., 1999). Our data support a potential mechanism by which the regulatory link between DNMT and p21 does not rely on changes of p21 DNA methylation.

Our results demonstrated that 3 μM BpV remarkably inhibited HT22 cell proliferation, as cells were arrested in S phase; simultaneously, DNMTs were increased. However, the exact mechanism by which BpV induced DNMTs still requires further exploration. In the meantime, BpV may be considered as an agent for activating DNMTs in HT22 cells.

Author contributions: *Study concept: GS, CYZ and SCY; experiment implementation: XLT, SYJ, and XLZ; data analysis: JY, JHC and XLL; manuscript preparation: KRG. All authors approved the final version of the paper.*
Conflicts of interest: *The authors declare that there are no conflicts of interest associated with this manuscript.*
Financial support: *This study was supported by the National Natural Science Foundation of China, No. 81160244, 81360316, 81460283, 81660307 (all to GS); the Inner Mongolia Science Foundation of China, No. 2018LH08078 (to GS), 2016MS(LH)0307 (to SYJ); the Baotou Health Foundation, China, No. WSJJ2016008 (to SYJ); the Inner Mongolia Educational Research Foundation, China, No. NJZY207 (to GS), NJZY17243 (to SCY), NJZY17250 (to XLL), NJZY17251 (to SYJ); the Baotou Medical College Foundation, China of No. BYJJ-DF201602, BYJJ-YF201615, BSJJ201617, BYJJ-QM201633, BYJJ-QM201656, BYJJ201502 (to GS); the Science and Technology Planning Project of Baotou of China, No. CX2017-5 (to GS); the National Key R&D Program of China, No. 2017YFC1308405 (to GS). The funding sources had no role in study conception and design, data analysis or interpretation, paper writing or deciding to submit this paper for publication.*
Copyright license agreement: *The Copyright License Agreement has been signed by all authors before publication.*
Data sharing statement: *Datasets analyzed during the current study are available from the corresponding author on reasonable request.*
Plagiarism check: *Checked twice by iThenticate.*
Peer review: *Externally peer reviewed.*

References

Alelu-Paz R, Gonzalez-Corpas A, Ashour N, Escanilla A, Monje A, Guerrero Marquez C, Algora Weber M, Ropero S (2014) DNA methylation pattern of gene promoters of major neurotransmitter systems in older patients with schizophrenia with severe and mild cognitive impairment. Int J Geriatr Psychiatry 30:558-565.

Andrezalova L, Gbelcova H, Durackova Z (2013) DNA damage induction and antiproliferative activity of vanadium(V) oxido monoperoxido complex containing two bidentate heteroligands. J Trace Elem Med Biol 27:21-26.

Bestor TH (2000) The DNA methyltransferases of mammals. Hum Mol Genet 9:2395-2402.

Bettscheider M, Kuczynska A, Almeida O, Spengler D (2012) Optimized analysis of DNA methylation and gene expression from small, anatomically-defined areas of the brain. J Vis Exp doi:10.3791/3938.

Bevan AP, Drake PG, Yale JF, Shaver A, Posner BI (1995) Peroxovanadium compounds: biological actions and mechanism of insulin-mimesis. Mol Cell Biochem 153:49-58.

Bieger S, Morinville A, Maysinger D (2002) Bisperoxovanadium complex promotes dopamine exocytosis in PC12 cells. Neurochem Int 40:307-314.

Bohmer RM (1982) Flow cytometry and cell proliferation kinetics. Prog Histochem Cytochem 14:1-62.

Caron D, Savard PE, Doillon CJ, Olivier M, Shink E, Lussier JG, Faure RL (2008) Protein tyrosine phosphatase inhibition induces anti-tumor activity: evidence of Cdk2/p27 kip1 and Cdk2/SHP-1 complex formation in human ovarian cancer cells. Cancer Lett 262:265-275.

Cassinotti E, Melson J, Liggett T, Melnikov A, Yi Q, Replogle C, Mobarhan S, Boni L, Segato S, Levenson V (2012) DNA methylation patterns in blood of patients with colorectal cancer and adenomatous colorectal polyps. Int J Cancer 131:1153-1157.

Cerovac Z, Ban J, Morinville A, Yaccato K, Shaver A, Maysinger D (1999) Activation of MAPK by potassium bisperoxo (1,10-phenanthroline) oxovanadate (V). Neurochem Int 34:337-344.

Chakrabarty S, Banerjee R (2016) Oxidation of L-Methionine by Bisperoxo (1,10-phenanthroline) oxovanadate (V): a mechanistic study. Int J Chem Kinet 48:274-280.

Cheng Y, Yan Z, Liu Y, Liang C, Xia H, Feng J, Zheng G, Luo H (2014) Analysis of DNA methylation patterns associated with the gastric cancer genome. Oncol Lett 7:1021-1026.

Eyvani H, Moghaddaskho F, Kabuli M, Zekri A, Momeny M, Tavakkoly-Bazzaz J, Alimoghaddam K, Ghavamzadeh A, Ghaffari SH (2016) Arsenic trioxide induces cell cycle arrest and alters DNA methylation patterns of cell cycle regulatory genes in colorectal cancer cells. Life Sci 167:67-77.

Fang JY, Lu YY (2002) Effects of histone acetylation and DNA methylation on p21(WAF1) regulation. World J Gastroenterol 8:400-405.

Faure R, Vincent M, Dufour M, Shaver A, Posner BI (1995) Arrest at the G2/M transition of the cell cycle by protein-tyrosine phosphatase inhibition: studies on a neuronal and a glial cell line. J Cell Biochem 59:389-401.

Fournel M, Sapieha P, Beaulieu N, Besterman JM, MacLeod AR (1999) Down-regulation of human DNA-(cytosine-5) methyltransferase induces cell cycle regulators p16 (ink4A) and p21 (WAF/Cip1) by distinct mechanisms. J Biol Chem 274:24250-24256.

Gibbs JR, van der Brug MP, Hernandez DG, Traynor BJ, Nalls MA, Lai SL, Arepalli S, Dillman A, Rafferty IP, Troncoso J, Johnson R, Zielke HR, Ferrucci L, Longo DL, Cookson MR, Singleton AB (2010) Abundant quantitative trait loci exist for DNA methylation and gene expression in human brain. PLoS Genet 6:e1000952.

He M, Liu J, Cheng S, Xing Y, Suo WZ (2013) Differentiation renders susceptibility to excitotoxicity in HT22 neurons. Neural Regen Res 8:1297-1306.

Hwang JY, Choi SC, Park JH, Kang SW (2011) The use of green tea extract as a storage medium for the avulsed tooth. J Endod 37:962-967.

Irving E, Stoker AW (2017) Vanadium Compounds as PTP Inhibitors. Molecules 22:E2269.

Jiemjit A, Fandy TE, Carraway H, Bailey KA, Baylin S, Herman JG, Gore SD (2008) p21(WAF1/CIP1) induction by 5-azacytosine nucleosides requires DNA damage. Oncogene 27:3615-3623.

Jung KH, Torrone D, Lovinsky-Desir S, Perzanowski M, Bautista J, Jezioro JR, Hoepner L, Ross J, Perera FP, Chillrud SN, Miller RL (2017) Short-term exposure to PM2.5 and vanadium and changes in asthma gene DNA methylation and lung function decrements among urban children. Respir Res 18:63.

Kioseoglou E, Petanidis S, Gabriel C, Salifoglou A (2015) The chemistry and biology of vanadium compounds in cancer therapeutics. Coord Chem Rev 301-302:87-105.

Levina A, Lay PA (2017) Stabilities and biological activities of vanadium drugs: what is the nature of the active species? Chem Asian J 12:1692-1699.

Li Q, Li J, Wen T, Zeng W, Peng C, Yan S, Tan J, Yang K, Liu S, Guo A, Zhang C, Su J, Jiang M, Liu Z, Zhou H, Chen X (2014) Overexpression of HMGB1 in melanoma predicts patient survival and suppression of HMGB1 induces cell cycle arrest and senescence in association with p21 (Waf1/Cip1) up-regulation via a p53-independent, Sp1-dependent pathway. Oncotarget 5:6387-6403.

Liu Y, Sun L, Fong P, Yang J, Zhang Z, Yin S, Jiang S, Liu X, Ju H, Huang L, Bai J, Gong K, Yan S, Zhang C, Shao G (2017) An association between overexpression of DNA methyltransferase 3B4 and clear cell renal cell carcinoma. Oncotarget 8:19712-19722.

Lou J, Wang Y, Yao C, Jin L, Wang X, Xiao Y, Wu N, Song P, Song Y, Tan Y, Gao M, Liu K, Zhang X (2013) Role of DNA methylation in cell cycle arrest induced by Cr (VI) in two cell lines. PLoS One 8:e71031.

Matsugo S, Kanamori K, Sugiyama H, Misu H, Takamura T (2015) Physiological roles of peroxido-vanadium complexes: Leitmotif as their signal transduction pathway. J Inorg Biochem 147:93-98.

Miozzo F, Arnould H, de Thonel A, Schang AL, Saberan-Djoneidi D, Baudry A, Schneider B, Mezger V (2018) Alcohol exposure promotes DNA methyltransferase DNMT3A upregulation through reactive oxygen species-dependent mechanisms. Cell Stress Chaperones 23:115-126.

Mytych J, Zebrowski J, Lewinska A, Wnuk M (2017) Prolonged effects of silver nanoparticles on p53/p21 pathway-mediated proliferation, DNA damage response, and methylation parameters in HT22 hippocampal neuronal cells. Mol Neurobiol 54:1285-1300.

Nakashima S, Arnold SA, Mahoney ET, Sithu SD, Zhang YP, D'Souza SE, Shields CB, Hagg T (2008) Small-molecule protein tyrosine phosphatase inhibition as a neuroprotective treatment after spinal cord injury in adult rats. J Neurosci 28:7293-7303.

Okano M, Bell DW, Haber DA, Li E (1999) DNA methyltransferases Dnmt3a and Dnmt3b are essential for de novo methylation and mammalian development. Cell 99:247-257.

Posner BI, Faure R, Burgess JW, Bevan AP, Lachance D, Zhang-Sun G, Fantus IG, Ng JB, Hall DA, Lum BS (1994) Peroxovanadium compounds. A new class of potent phosphotyrosine phosphatase inhibitors which are insulin mimetics. J Biol Chem 269:4596-4604.

Prowse DM, Bolgan L, Molnar A, Dotto GP (1997) Involvement of the Sp3 transcription factor in induction of p21Cip1/WAF1 in keratinocyte differentiation. J Biol Chem 272:1308-1314.

Rodriguez-Osorio N, Wang H, Rupinski J, Bridges SM, Memili E (2010) Comparative functional genomics of mammalian DNA methyltransferases. Reprod Biomed Online 20:243-255.

Saradalekshmi KR, Neetha NV, Sathyan S, Nair IV, Nair CM, Banerjee M (2014) DNA methyl transferase (DNMT) gene polymorphisms could be a primary event in epigenetic susceptibility to schizophrenia. PLoS One 9:e98182.

Shao G, Zhang R, Zhang S, Jiang S, Liu Y, Zhang W, Zhang Y, Li J, Gong K, Hu XR, Jiang SW (2013) Splice variants DNMT3B4 and DNMT3B7 overexpression inhibit cell proliferation in 293A cell line. In Vitro Cell Dev Biol Anim 51:210.

Stephens C, Reisenauer A, Wright R, Shapiro L (1996) A cell cycle-regulated bacterial DNA methyltransferase is essential for viability. Proc Natl Acad Sci U S A 93:1210-1214.

Taberlay PC, Jones PA (2011) DNA methylation and cancer. Prog Drug Res 67:1-23.

Tasdogan A, Kumar S, Allies G, Bausinger J, Beckel F, Hofemeister H, Mulaw M, Madan V, Scharfetter-Kochanek K, Feuring-Buske M, Doehner K, Speit G, Stewart AF, Fehling HJ (2016) DNA damage-induced HSPC malfunction depends on ROS accumulation downstream of IFN-1 signaling and Bid mobilization. Cell Stem Cell 19:752-767.

Wu Q, Ni X (2015) ROS-mediated DNA methylation pattern alterations in carcinogenesis. Curr Drug Targets 16:13-19.

Xiong H, Chen ZF, Liang QC, Du W, Chen HM, Su WY, Chen GQ, Han ZG, Fang JY (2009) Inhibition of DNA methyltransferase induces G2 cell cycle arrest and apoptosis in human colorectal cancer cells via inhibition of JAK2/STAT3/STAT5 signalling. J Cell Mol Med 13:3668-3679.

Yang J, Zhang Z, Jiang S, Zhang M, Lu J, Huang L, Zhang T, Go ng K, Yan S, Yang Z, Shao G (2016) Vanadate-induced antiproliferative and apoptotic response in esophageal squamous carcinoma cell line EC109. J Toxicol Environ Health A 79:864-868.

Yang J, Tian X, Yang J, Cui J, Jiang S, Shi R, Liu Y, Liu X, Xu W, Xie W, Jia X, Bade R, Zhang T, Zhang M, Gong K, Yan S, Yang Z, Shao G (2017) 5-Aza-2'-deoxycytidine, a DNA methylation inhibitor, induces cytotoxicity, cell cycle dynamics and alters expression of DNA methyltransferase 1 and 3A in mouse hippocampus-derived neuronal HT22 cells. J Toxicol Environ Health A 80:1222-1229.

Yang P, Dankowski A, Hagg T (2007) Protein tyrosine phosphatase inhibition reduces degeneration of dopaminergic substantia nigra neurons and projections in 6-OHDA treated adult rats. Eur J Neurosci 25:1332-1340.

Yu JY, Lee JJ, Jung JK, Kim TJ, Yoo HS, Yun YP, Lee JC (2009) JY0691, a newly synthesized obovatol derivative, inhibits cell cycle progression of rat aortic smooth muscle cells through up-regulation of p21 (cip1). Eur J Pharmacol 624:23-30.

Yu L, Dawe RJ, Boyle PA, Gaiteri C, Yang J, Buchman AS, Schneider JA, Arfanakis K, De Jager PL, Bennett DA (2017) Association between brain gene expression, DNA methylation, and alteration of ex vivo magnetic resonance imaging transverse relaxation in late-life cognitive decline. JAMA Neurol 74:1473-1480.

Zhang S, Zhang Y, Jiang S, Liu Y, Huang L, Zhang T, Lu G, Gong K, Ji X, Shao G (2014) The effect of hypoxia preconditioning on DNA methyltransferase and PP1gamma in hippocampus of hypoxia preconditioned mice. High Alt Med Biol 15:483-490.

Zhang Z, Yang J, Liu X, Jia X, Xu S, Gong K, Yan S, Zhang C, Shao G (2016) Effects of 5-Aza-2'-deoxycytidine on expression of PP1gamma in learning and memory. Biomed Pharmacother 84:277-283.

Zhao Z, Lu R, Zhang B, Shen J, Yang L, Xiao S, Liu J, Suo WZ (2016) Differentiation of HT22 neurons induces expression of NMDA receptor that mediates homocysteine cytotoxicity. Neurol Res 34:38-43.

Zurlo D, Leone C, Assante G, Salzano S, Renzone G, Scaloni A, Foresta C, Colantuoni V, Lupo A (2013) Cladosporol a stimulates G1-phase arrest of the cell cycle by up-regulation of p21 (waf1/cip1) expression in human colon carcinoma HT-29 cells. Mol Carcinog 52:1-17.

C-Editor: Zhao M; S-Editors: Wang J, Li CH; L-Editors: Deusen AV, Hindle A, Qiu Y, Song LP; T-Editor: Liu XL